

Analysis of glass forming ability using percolation concept and tunability of physical parameters of a-Ge₁₂Se_{76-x}As₁₂Bi_x glassy semiconductors

ISHU SHARMA*, SRUTHI SUNDER

Department of Physics, Amity University Dubai, Dubai International Academic City, United Arab Emirates

Glass forming ability of lone-pair semiconductors was analyzed for ($x = 0, 2, 4, 6, 8, 10$) system. Values of lone pair electrons L were calculated using average coordination number of valence electrons. These values were found to decrease, as the system was moving towards the rigid region. $L > 3$ values showed vitreous state. Deviation of the stoichiometry confirmed the chalcogen-rich region. A linear correlation was found between the mean bond energy and glass transition temperature. Chemical Bond Approach model was applied to calculate the cohesive energy of the system. A linear relationship was found to exist between the cohesive energy and the theoretical band gap, calculated using Shimakawa relation. A decrease in both parameters was explained on the basis of average stabilization energy and electronegativity of the system. The density values were found to increase and may account for higher refractive index of the system. Large Bohr radius of the Bi atom accounted for an increase in the polarizability. Other parameters *viz.* degree of covalency, packing density, compactness, molar volume, free volume percentage, excess volume and polaron radius were also calculated. An effort was made to correlate the effect of Bi addition to Ge₁₂Se_{76-x}As₁₂Bi_x lone-pair semiconductor on the basis of the structure of the glassy matrix or the connectedness of the material.

Keywords: constraints; glass transition temperature; band gap; cohesive energy

1. Introduction

Semiconductor technology is challenged to develop next generation materials for potential usage and demanding applications. In this regard, chalcogenide glasses attract considerable scientific interest as a result of their exciting optical characteristics. Chalcogenide glasses are low-phonon energy materials and usually have a wide transparent window from the visible up to infrared region. They have a distinct place in the field of optoelectronics and technically significant applications in solid-state devices, plasmonics, nanotechnology, etc. Higher linear refractive index, third order nonlinear refractive index and substantial absorption in visible to NIR part of the spectrum make them irreplaceable materials for mid-infrared sensing, integrated optics and ultrahigh-bandwidth signal processing. Thin films of chalcogenide glasses are

promising materials for high-resolution, grayscale photo- and electron-beam resists for nanoscale and ultrathin applications in MEMS/NEMS technology. Their applications as phase change memories (DVDs), X-ray medical image sensors, highly sensitive vidicons, holographic memories, nonlinear devices, solar cells, and ionic devices have been reported [1–5]. Among the chalcogens, Se has extensive device applications, such as switching memory, xerography, optical memory devices, etc. It also exhibits a unique property of reversible transformation [6]. The Ge–Se is a broadly studied system. Ge atoms act as bond modifiers when added with Se. Ge strengthens the average bond by cross-linking the Se chain structure and increases the glass transition temperature and resistivity [7]. It also overcomes some difficulties of pure Se, such as short lifetime and low sensitivity. Also, the addition of the third element to Ge–Se alloys can further improve their properties and make them a more appropriate candidate for various applications.

*E-mail: ishuphy@gmail.com

The effect of indium addition on Ge–Se glassy alloys was studied by the author for its optical (linear and non-linear), electrical and physical properties previously [8, 9]. Chalcogens can be doped by many elements. Hence, their properties can be tailored. They are of interest in order to understand their structure, properties and the need to assess their potential technological applications. In the present manuscript, authors decided to keep Ge–Se–As as a parent matrix because all its components have similar size and electronegativity. Therefore, this results in a close-to-ideal covalent network [10]. The addition of As (arsenic) to Ge–Se matrix broadens glass formation region. Due to more flexible structure, arsenic addition gives hundreds of times higher optical non-linearity and higher sensitivity to irradiation [11]. Its thermomechanical properties make it easy to be moulded into sophisticated diffractive and aspheric lenses. Highly nonlinear fibre is used for applications which include supercontinuum generation, frequency metrology, and wavelength conversion [12, 13]. Commercial chalcogenide glasses, such as AMTIR-1 (As 12 at.%) and GASIR1, are also produced from this system [14]. The addition of Bi to the Ge–Se system increases the chemical durability and broadens the IR transparency region. The replacement of Se with Bi in Ge–Se host matrix leads to the decrease in the activation energy and exhibits electronic switching. Bi facilitates n-type conduction as a carrier-type reversal, i.e. $p \rightarrow n$ transition [15]. Investigation of physical parameters of any system is useful to those engaged in experimental research and development of these materials. In the present work, the composition was chosen to help avoid nanophase separation [16]. With high germanium content, refractive index (linear and non-linear) drops down. Thus, Ge is kept at 12 at.%. It has been observed that the crystallization ability of the glasses increases with an addition of Bi. The glasses partially crystallize when Bi goes beyond 13 at.% [17]. It has been reported that when the Ge content is 20 at.%, the maximum of Bi content which can be incorporated into the Ge–Se matrix, is only 13 at.% [18]. Moreover, with the increase in Bi content from 0 to 10 at.%, a sharp change is observed in optical band

gap and electrical activation energy, approximately around 8 at.% to 9 at.% of Bi [19, 20]. The composition at lower Bi content exhibits luminescence, while the composition showing n-type conduction fails to exhibit it [21].

Therefore, in the present manuscript the authors decided to study and discuss the compositional effect on the physical properties of $\text{Ge}_{12}\text{Se}_{76-x}\text{As}_{12}\text{Bi}_x$ ($x = 0, 2, 4, 6, 8, 10$) glassy alloys. Average coordination number and a total number of constraints were investigated using topological concepts. Correlation between the glass transition temperature and mean bond energy was calculated. Other physical parameters, viz. lone pairs, glass forming ability, electronegativity, average heat of atomization, density, compactness, molar volume, free volume percentage, cohesive energy and theoretical band gap were also calculated. An effort was made to correlate these parameters in terms of composition, bond strength, bond energies or equivalently with an average coordination number $\langle r \rangle$.

2. Theoretical considerations

Theoretical study was done on the physical properties of Ge–Se–As–Bi system with the variation of Bi content. Continuous random network models were used to illustrate the structure of the glasses. Deviation from stoichiometry, mean bond energy and glass transition temperature were calculated using Tichy-Ticha approach. Theoretical band gap was evaluated using Shimakawa relation. Chemical bond approach model was used to show the chemical distribution of bonds and to evaluate the overall energy of the system. Electronegativity of the system was calculated from Sander-son principle. Using density values, calculated using Fayek relationship, molar volume, compactness and other relevant parameters were also calculated. Naster-Kingery formula was applied to calculate Se atomic density. The later is used to calculate polaron radius.

3. Result and discussion

3.1. Nearest neighbor coordination

Ioffe et al. [22] put forward the concept of bonding nature in the nearest neighbor region, known as the coordination number. It is particularly suitable for testing the validity of topological concepts in a ternary system due to its large glass forming region [23]. It obeys the 8-N rule, where N is the valency of an atom. In relevance with this coordination number, the bonding character in the nearest neighbor region characterizes the electronic properties of semiconductor materials. The nearest neighbor coordination or the average coordination number was determined by the formula:

$$\langle r \rangle = \frac{aX + bY + cZ + d\delta}{a + b + c + d} \quad (1)$$

where a, b, c and d are the at.% of Ge, Se, As, and Bi, and X = 4, Y = 2, Z = 3 and $\delta = 3$ are their respective coordination numbers. The obtained values of $\langle r \rangle$ for $\text{Ge}_{12}\text{Se}_{76-x}\text{As}_{12}\text{Bi}_x$ ($x = 0, 2, 4, 6, 8, 10$) are shown in Table 1. In chalcogenide glasses, the covalent network constrained by bond bending and bond stretching has a critical connectivity threshold at $\langle r \rangle = 2.4$. A covalently bonded glassy network consisting of $N = \sum n_i$ atoms is greatly influenced by mechanical constraints N_{con} . This is given by the sum of bond bending N_α and bond stretching N_β forces as: $N_{\text{con}} = N_\alpha + N_\beta$ where $N_\alpha = \frac{\sum n_i r_i}{2}$ and $N_\beta = \sum n_i (2r_i - 3)$. The investigation of constraints for a covalently bonded matrix helps us to reveal numerous substructures and mechanical softening of the network. According to the constraint theory, chalcogenide glasses can be classified into three types as: (i) floppy or under-coordinated bonds with $\langle r \rangle < 2.4$ and $N_{\text{con}} < 3$ (polymeric glass with isolated rigid regions); (ii) optically coordinated and at a mechanically critical point with $\langle r \rangle = 2.4$ and $N_{\text{con}} = 3$; (iii) rigid and over coordinated (where the rigidity percolates) with $\langle r \rangle > 2.4$ and $N_{\text{con}} > 3$ [24]. According to the constraint model and development theories [25], on equating the number of operative constraints to the number of degree of freedom, inferring that for the most stable glass, the $\langle r \rangle$ value is approximately 2.4. This $\langle r \rangle$ value is referred as the rigidity

percolation or mechanical threshold. In the system under investigation, $\langle r \rangle$ varies from 2.36 to 2.46. This increase in $\langle r \rangle$ can be explained by the replacement of two-fold Se chains or Se rings with three-fold Bi atoms. Also, values of N_{con} are increasing from 2.9 to 3.15 (Table 1). It is clear from the tabulated values that for Bi = 4 at.%, $\langle r \rangle$ and N_{con} approach 2.4 and 3, respectively. Hence, $\text{Ge}_{12}\text{Se}_{72}\text{As}_{12}\text{Bi}_4$ is theoretically the most stable composition under investigation. It lies almost at the threshold of the mode change, i.e. moving from under-coordinated to optically coordinated and finally to optically over-coordinated mode. According to Thorpe [26], the number of floppy modes is given by $M_f = 2 - \frac{5\langle r \rangle}{6}$. Reduction in M_f from 0.03 to -0.05 with increasing Bi content, indicates that the system is moving towards a more rigid region. The values of cross-linking density (D_{CL}) [27] were calculated as ($D_{\text{CL}} = N_{\text{con}} - 2$) and are found to increase. The effective coordination number $\langle r_{\text{eff}} \rangle$ was calculated using $\langle r_{\text{eff}} \rangle = \frac{2}{5}N_{\text{con}} + 3$ and is increasing with an increasing Bi content as seen in Table 1. Thus, from the calculated data, we can infer that with the increase in Bi content, Ge-Se-As-Bi matrix is heading from floppy to rigid modes.

3.2. Relation between glass forming ability and lone pair electrons of the structure

Lone-pair electrons are found in chalcogenide glasses (ChG) and are located in the valence band. Therefore, ChG can also be referred as lone-pair glass semiconductor. Within this glass formation, a significant role is played by the lone-pair electrons and implicit in terms of valence shell electron pair repulsion theory. According to Fouad et al. [28] raising the number of lone-pair electrons in a composition reduces the strain energy in a network. Consequently, a composition which possesses a large number of lone-pair electrons must support good glass formation. Therefore, a steady state can be attained merely if sufficient lone-pair electrons exist in the system, which contributes to the thermal stability. Many substances which solidify in the vitreous state are found to contain structural ‘bridges’.

Table 1. Values of average coordination number ($\langle r \rangle$), bond bending (N_α), bond stretching forces (N_β), total number of constraints (N_{con}), number of floppy modes (M_f), cross-linking density (D_{CL}), effective coordination number ($\langle r_{\text{eff}} \rangle$), valence electrons (V) and lone pair electrons (L) with Bi at.% for $\text{Ge}_{12}\text{Se}_{76-x}\text{As}_{12}\text{Bi}_x$ ($x = 0, 2, 4, 6, 8, 10$) system.

x	$\langle r \rangle$	N_α	N_β	N_{con}	M_f	D_{CL}	$\langle r_{\text{eff}} \rangle$	V	$L = V - \langle r \rangle$
0	2.36	1.18	1.72	2.9	0.033	0.89	2.36	5.64	3.28
2	2.38	1.19	1.76	2.95	0.017	0.95	2.38	5.62	3.24
4	2.40	1.20	1.80	3.00	0	1.00	2.40	5.60	3.20
6	2.42	1.21	1.84	3.05	-0.016	1.05	2.42	5.58	3.16
8	2.44	1.22	1.88	3.1	-0.034	1.10	2.44	5.56	3.12
10	2.46	1.23	1.92	3.15	-0.050	1.15	2.46	5.54	3.08

These give rise to linear, bi-dimensional or tri-dimensional hetero polymeric formations. In most glasses, the bridges are formed by group VI and VII elements. Se atoms in glass structures also have two pairs of lone-pair electrons. The existence of bridging atoms with lone-pair electrons can decrease the strain forces and possess a character of flexibility. These strain forces are caused by the formation of amorphous materials and chemical bonds with lone-pair electrons. Hence, structures with large numbers of lone-pair electrons favor vitreous state. Lone pair electrons (L) in a chalcogenide glass system were calculated as $L = V - \langle r \rangle$, with the preamble of $\langle r \rangle$ proposed by Phillips [25]. Here, V is the number of valence electrons which is equal to unshared lone-pair electrons and is tabulated in Table 1. It is seen that the number of lone-pair electrons decreases with an increase of Bi content in the system. This may be attributed to the decrease in flexibility of the system and can explain the interaction between Bi and the lone pair electrons of a bridging Se atom. This decrease in the L value shows that the system's strain energy increases. The bonds are tough to deform and are directing towards the intermediate region. This can be further confirmed by the increase in $\langle r \rangle$ values as shown in Fig. 1.

Liang [29] linked the ability of a chalcogenide system to maintain its vitreous state, with the number of lone pair electrons. According to Liang theory, L should be greater than 3. Observing the tabulated L values (3.28 to 3.08), our system is in well-defined range. Apart from the lone pair electron

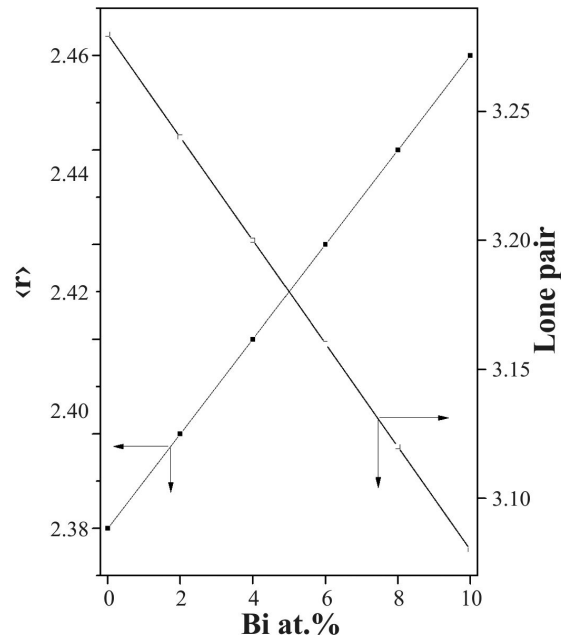


Fig. 1. Variation of average coordination number and lone pair with Bi at.% for $\text{Ge}_{12}\text{Se}_{76-x}\text{As}_{12}\text{Bi}_x$ ($x = 0, 2, 4, 6, 8, 10$) glassy alloys.

calculations, there are also other factors which majorly decide on both glass formation and thermal stability. The key role is played by kinetic temperatures of glass transition and crystallization [30].

3.3. Correlation between mean bond energy $\langle E \rangle$ and glass transition temperature T_g

Glass transition temperature T_g represents the temperature above which an amorphous matrix can attain various structural configurations and below

which the matrix is frozen into a structure that cannot easily change to another form. The value of T_g is directly related to the energy required to break and reform the covalent bonds of the amorphous composition or any random network. Hence, it is reasonable to assume that T_g must be related to the magnitude of the cohesive forces within the network. These forces must be overcome to allow the atom movement. The predictions of T_g are generally based on simple models. According to chemical bond ordering model, it is assumed that T_g is proportional to mean bond energy. This energy strongly depends on the cohesive forces or rigidity of the network. Thorpe et al. [31] also recognized that T_g is not only related to the connectedness of the network $\langle r \rangle$ but besides this holds an excellent empirical correlation with mean bond energy $\langle E \rangle$ of the system. They examined about 200 chalcogenide glasses by taking into account all of the above-mentioned factors in a range from 320 K to 760 K. This led to obtaining a good correlation between T_g and $\langle E \rangle$, i.e. $T_g = 311(\langle E \rangle - 0.9)$.

In Ge–Se–As–Bi system, there is a significant difference between the bonding energies of heteropolar bonds (i.e. Ge–Se, As–Se and Bi–Se) and of homopolar bonds (i.e. Se–Se and Bi–Bi). Thus, a chemically ordered network is expected. This model does not account for the molecular interactions. These interactions play a vital role in the relaxation process in the glass transition region and are considered as the major limitation.

The overall mean bond energy $\langle E \rangle$ gives us an important parameter which is closely related to several properties of chalcogenide glasses. It is a function of average coordination number as well as different types of energy involved in glass formation. Based on the theory developed by Tichý et al. [32], the mean bond energy is given by $\langle E \rangle = \bar{E}_c + \bar{E}_{rm}$ where \bar{E}_c is the average energy of cross-linking per atom. \bar{E}_{rm} refers to the contribution arising from weaker bonds that remain after the strong bonds have been maximized, i.e. the average bond energy per atom of the remaining matrix. Values of E_c and E_{rm} further depend on the values of R .

R is a parameter that determines the deviation from stoichiometry. It is expressed by the ratio of covalent bonding possibilities of chalcogen atom to the non-chalcogen atom. $R < 1$, indicates a chalcogen-rich material which consists of both heteropolar bonds and chalcogen-chalcogen bonds. $R < 1$, indicates a chalcogen-poor material consisting of heteropolar and metal-metal bonds. $R = 1$ is indicative of stoichiometric composition containing only heteropolar bonds. It basically shows the minimum chalcogen content at which a chemically ordered network is formed. For the $\text{Ge}_{12}\text{Se}_{76-x}\text{As}_{12}\text{Bi}_x$ system the R was calculated using the formula:

$$R = \frac{(76-x)\langle r \rangle(\text{Se})}{12\langle r \rangle(\text{Ge}) + 12\langle r \rangle(\text{As}) + x\langle r \rangle(\text{Bi})} \quad (2)$$

The calculated values of R are given in Table 2. The R values for each composition are greater than unity indicating a chalcogens-rich material having heteropolar and chalcogenide-chalcogenide bonds. Depending upon the deviation from stoichiometry:

$$\bar{E}_c = P_p E_{hb} \text{ for } R < 1 \text{ and } \bar{E}_c = P_r E_{hb} \text{ for } R > 1 \quad (3)$$

where E_{hb} is the average heteropolar bond energy for glasses with composition $\text{Ge}_\alpha\text{Se}_\beta\text{As}_\gamma\text{Bi}_\delta$. It was calculated as:

$$E_{hb} = \frac{\alpha\langle r \rangle(\text{Ge})E_{\text{Ge-Se}} + \gamma\langle r \rangle(\text{As})E_{\text{As-Se}} + \delta\langle r \rangle(\text{Bi})E_{\text{Bi-Se}}}{\alpha\langle r \rangle(\text{Ge}) + \gamma\langle r \rangle(\text{As}) + \delta\langle r \rangle(\text{Bi})} \quad (4)$$

where $E_{\text{Ge-Se}}$, $E_{\text{As-Se}}$, and $E_{\text{Bi-Se}}$ are the heteropolar bond energies for Ge–Se, As–Se and Bi–Se, respectively (Table 2). The degrees of cross-linking/atom P_p (for $R < 1$) and P_r (for $R > 1$) were calculated as:

$$P_p = \frac{\beta\langle r \rangle(\text{Se})}{\alpha + \beta + \gamma + \delta} \quad (5)$$

and

$$P_r = \frac{\alpha\langle r \rangle(\text{Ge}) + \gamma\langle r \rangle(\text{As}) + \delta\langle r \rangle(\text{Bi})}{\alpha + \beta + \gamma + \delta} \quad (6)$$

The average bond energy per atom of the remaining matrix (\bar{E}_{rm}) was given as:

$$\bar{E}_{rm} = \frac{2(0.5\langle r \rangle - P_p)E_{\langle \rangle}}{\langle r \rangle} \quad (7)$$

where:

$$E_{\langle \rangle} = \frac{E_{Ge-Ge} + E_{As-As} + E_{Bi-Bi}}{3} \text{ (for } R < 1) \quad (8)$$

and

$$E_{rm} = \frac{2(0.5\langle r \rangle - P_r)}{\langle r \rangle} E_{Se-Se} \text{ (for } R > 1) \quad (9)$$

Using $\langle E \rangle = \bar{E}_c + \bar{E}_{rm}$ and $T_g = 311(\langle E \rangle - 0.9)$, both mean bond energy and glass transition temperature values were predicted and tabulated in Table 2. With an increase in Bi content in the Ge–Se–As–Bi glassy alloy, both mean bond energy and glass transition temperature show an increase and reach a maximum at the chemical threshold, $R \approx 1$ (Table 2 and Fig. 2).

Equations $\langle E \rangle = 51.09 + 0.273x$ kcal/g-atom and $T_g = 41.03 + 3.71x$ K show the empirical relations of both $\langle E \rangle$ and T_g , respectively, with an increase in Bi content. In particular, the compositional dependence of T_g in numerous glassy systems presents maximum value near to the chemical threshold (i.e. $R = 1$). This is also the point of existence of predominance of heteropolar bonds which is also evident from chemical bond distribution given in Table 3 (calculated in the next section). This marks the minimum Se content at which a chemically ordered network is possible without metal-metal bond formation.

From the tabulated values, it is found that T_g increases with an increase in rigidity of the system, degree of cross linking and average bond strength. Hence, we interpret that the observed variation of glass transition temperature with Bi content is due to the dependence of T_g on the connectivity [33]. Inset in Fig. 2 also shows an increase in density with an increase in Bi at.% (calculated later). A linear relationship between density and glass transition temperature is also experimentally proved in the literature [34].

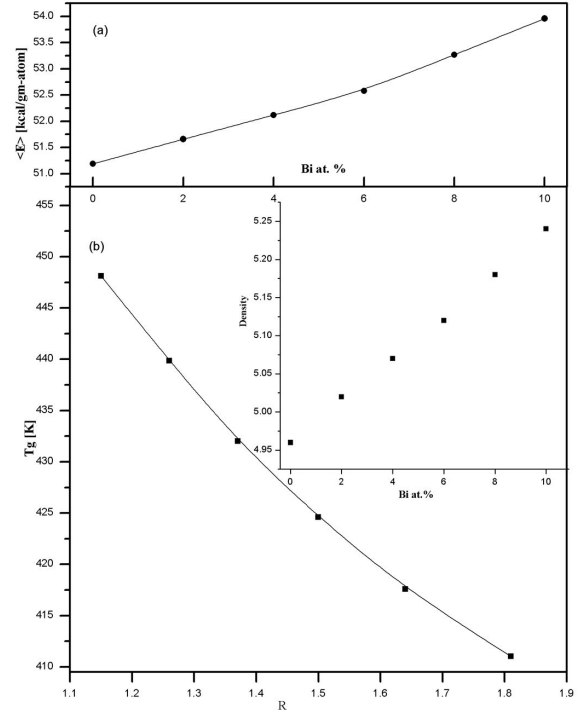


Fig. 2. Variation of (a) mean bond energy $\langle E \rangle$ with Bi at.% (b) glass transition temperature T_g with R and inset of Fig. 2b shows variation of density [g/cc] with Bi at.% for $Ge_{12}Se_{76-x}As_{12}Bi_x$ ($x = 0, 2, 4, 6, 8, 10$) glassy alloys.

3.4. Correlation between cohesive energy (CE) and theoretical band gap (E_g^{th})

Physical properties of any composition depend on the chemical bonds of its constituents as well as the bond energies. The cohesive energy is the stabilization energy of an infinitely large cluster of material per atom. It also reflects the average bond strength. Therefore, a change in any property may be attributed to the changes in bond energy, bond angles or bond lengths [35, 36]. Explanation of many parameters of Ge–Se–As–Bi glasses can be given in terms of cohesive energy using the chemical bond approach (CBA) [37]. This assumption (generally found to be valid for glass structures) was used by Shaaban et al. [38] in his covalently bonded continuous random network model. This model also allows determining the number of possible bonds and their types, i.e. heteropolar or homopolar. According to CBA, heteropolar bonds

Table 2. Values of R, mean bond energy $\langle E \rangle$, glass transition temperature T_g and bond energies of the respective bonds in glassy $\text{Ge}_{12}\text{Se}_{76-x}\text{As}_{12}\text{Bi}_x$ ($x = 0, 2, 4, 6, 8, 10$) system.

x	R	$\langle E \rangle$ [kcal/g-atom]	T_g [K]	Bonds	Bond energy [kcal/mol]
0	1.81	51.19	411.03	Ge–Ge	37.60
2	1.64	51.66	417.59	Se–Se	44.0
4	1.50	52.12	424.59	Bi–Bi	25.0
6	1.37	52.58	432.02	Se–Bi	40.7
8	1.26	53.27	439.87	Ge–Se	49.10
10	1.14	53.96	448.12	Se–As	41.68

are favourable over homopolar bonds. Heteropolar bonds are formed in the sequence of decreasing bond energy until the available valence of atoms is satisfied. On using this assumption, bonds between similar atoms will only occur if there is an excess of a certain type of atoms. Furthermore, each constituent atom is coordinated by 8-N atoms. As a first approximation, CBA model neglects dangling bonds, other valence defects and van der Waals interactions, as they form much weaker links than regular covalent bonds. According to CBA, bond energies are assumed to be additive. The possible bonds in the a-Ge–Se–As–Bi system are Ge–Se, Se–As, Se–Bi, Se–Se and Bi–Bi. The variation of cohesive energy was studied as a function of Bi content and calculated by summing up the bond energies over all bonds expected in the material. Heteropolar bond energies were calculated as: $(A-B) = D(A-A) \cdot D(B-B)^{\frac{1}{2}} + 30(\chi_A - \chi_B)^2$ [27], where $D(A-A)$ and $D(B-B)$ are the homopolar bond energies of atoms A and B, respectively, and χ_A and χ_B are their respective electronegativities. Homopolar bond energies used to calculate heteropolar energies are tabulated in Table 2. Electronegativity values were taken from Pauling scale, i.e. $\chi_{\text{Ge}} = 2.01$, $\chi_{\text{Se}} = 2.55$, $\chi_{\text{As}} = 2.18$ and $\chi_{\text{Bi}} = 2.02$.

Knowing the bond energies, the cohesive energy values were derived by assuming the bond energies over the entire bonds expected in the system using equation $\text{CE} = \sum \frac{C_i D_i}{100}$ [39]. C_i and D_i are the number of expected chemical bonds and the energy of each corresponding bond, respectively. Calculated values of cohesive energy along with

chemical bond distribution for all compositions are tabulated in Table 3. The results indicate that the CE of these glassy alloys shows a decrease with an increasing Bi content (also shown in Fig. 3) as per the following empirical equation $\text{CE} = 45.03 - 0.0612x$ kcal/mol, where x is Bi at.%.

In the investigated network, Ge–Se bonds with highest bond energy are likely to form first. These bonds are probably saturating all the available valence of Ge. Therefore, all existing Ge is coupled with Se. The rest of the Se forms As–Se and Se–Bi bonds in the sequence of decreasing bond energy. After the formation of these bonds, there are still unsatisfied Se valences, satisfied by the formation of Se–Se homopolar defect bonds. With an increase in Bi content to Ge–Se–As–Bi matrix, the number of Se–Bi (40.7 kcal/mol) bonds increases, with lower bond energy, on an expense of Se–Se (44 kcal/mol). This decrease in the average bond energy presumably accounts for the decrease in the band gap of the system. The theoretical values of the energy gap E_g^{th} for quaternary alloys is given by the relation, $E_g^{\text{th}}(\text{ABCD}) = aE_g(A) + bE_g(B) + cE_g(C) + dE_g(D)$ where a , b , c and d are the volume fraction and $E_g(A)$, $E_g(B)$, and $E_g(C)$ are the optical gaps of A, B, C and D elements respectively. The conversion from volume fraction to atomic percentage is made by using atomic weight and density values. The values of E_g^{th} for all the compositions are also tabulated in Table 3. It is clear that with the Bi incorporation, theoretical band gap decreases from 1.77 eV to 1.55 eV. This decrease in E_g^{th} can

also attribute to the decrease in the cohesive energy or average stabilization energy of the system with the increase in Bi at.%. A subsequent decrease in electronegativity of the system is also found and is evident from Table 3 and inset of Fig. 3. The electronegativity of the system was calculated from Sanderson principle [40] $S = (\Pi S_{E,Z}^x)^{(\Sigma x)^{-1}}$, where x is at.% and $S_{E,Z}$ is the electronegativity of an individual atom. According to this principle, the electronegativity of the alloy is the geometric mean of electronegativity of its constituent elements. Mott et al. [41] model also accounts for the lowering of band gap with the Bi addition.

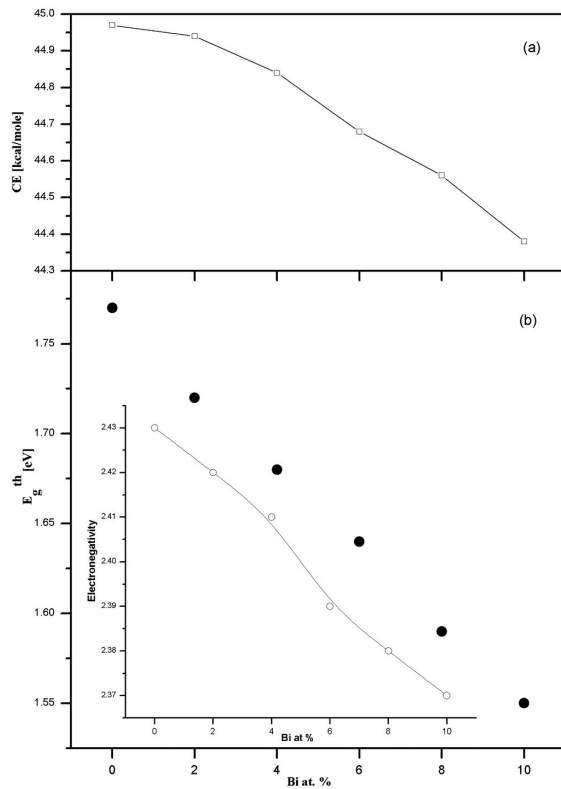


Fig. 3. Variation in (a) the cohesive energy (CE in kcal/mol) and (b) theoretical band gap (E_g^{th}) with Bi at.% and inset of Fig. 3b shows variation of electronegativity with Bi at.% for $Ge_{12}Se_{76-x}As_{12}Bi_x$ ($x = 0, 2, 4, 6, 8, 10$) glassy alloys.

The width of localized states near mobility edges depends on the degree of disorder and defects present in the system. An addition of Bi increases the degree of disorder in the alloy. Bi makes

bonds with Se and Bi–Se bonds introduce a large number of defects in the system [42]. Therefore, this increase in width of the localized states further accounts for the lowering of the band gap.

In order to complete the vision of the chemical bonds, it is appropriate to obtain the average heat of atomization H_S . The heat of atomization at standard temperature and pressure STP of a binary semiconductor formed from atoms A and B is the sum of the heat of formation and the average heats of atomization, respectively [27].

To extend this idea for ternary and higher order semiconductor compounds [43], the average heat of atomization H_S kcal/g-atom for $A\alpha B\beta C\gamma D\delta$ was calculated as:

$$H_S = \frac{\alpha H_S^A + \beta H_S^B + \gamma H_S^C + \delta H_S^D}{\alpha + \beta + \gamma + \delta} \quad (10)$$

where α , β , γ , and δ are the ratios of Ge, Se, As and Bi respectively. In the present system, the values of average heat of atomization (calculated by above equation) are tabulated in Table 3 and are found to decrease. The values of heat of atomization for Ge, Se, As and Bi atoms, have been taken as 89, 49, 72 and 49 in kcal/g-atom, respectively.

In ChG with high concentration of Se/Te, the valence band (σ -bonding) originates from lone pair electron states whereas the conduction band arises from antibonding states (σ^* -bonding) [44]. A linear correlation between the energy gap and the average heat of atomization exists as $\Delta E = a(H - b)$, where a and b are the characteristic constants [45]. H_S is a measure of cohesive energy and represents the relative bond strength. For the investigated matrix Ge–Se–As–Bi, $H_S/\langle r \rangle$ follows the given empirical relation $CE = 30.20 + 0.615H_S/\langle r \rangle$ kcal/g-atom, with CE.

Bond strength decreases with the consecutive decrease in H_S and the cohesive energy values. This reduction in bond strength causes less splitting between σ and σ^* , further resulting in the shrinkage of the band gap. Therefore, required-tunability of semiconducting alloys can be achieved through the compositional modulation [46].

Table 3. Values of electronegativity (χ), theoretical band gap E_g^{th} , distribution of chemical bonds, cohesive energy, heat of atomization (\bar{H}_S), and average heat of atomization ($\bar{H}_S/\langle r \rangle$) for the $\text{Ge}_{12}\text{Se}_{76-x}\text{As}_{12}\text{Bi}_x$ ($x = 0, 2, 4, 6, 8, 10$) system.

x	χ	E_g^{th} [eV]	Distribution of chemical bonds				Cohesive energy [kcal/mol]	\bar{H}_S [kcal/g-atom]	$\bar{H}_S/\langle r \rangle$ [kcal/g-atom]
			Ge-Se	As-Se	Bi-Se	Se-Se			
0	2.43	1.77	0.315	0.236	–	0.447	44.97	56.909	24.11
2	2.42	1.72	0.324	0.243	0.040	0.393	44.95	56.903	23.91
4	2.41	1.68	0.333	0.250	0.041	0.376	44.84	56.897	23.71
6	2.39	1.64	0.342	0.257	0.128	0.272	44.68	56.891	23.51
8	2.38	1.59	0.352	0.264	0.176	0.207	44.56	56.885	23.31
10	2.37	1.55	0.363	0.272	0.227	0.136	44.38	56.879	23.12

The degree of the covalency character C_C [47] of the different heteropolar bonds formed in the quaternary system was calculated using the following formula:

$$C_C = 100 \exp[-(\chi_A - \chi_B)^2/4] \quad (11)$$

where χ_A and χ_B are the electronegativities of atoms A and B. The calculated values of C_C are given in Table 4 and indicate that the covalent character of bonding is dominant in the parent sample.

Table 4. Values of covalence character for glassy $\text{Ge}_{12}\text{Se}_{76-x}\text{As}_{12}\text{Bi}_x$ ($x = 0, 2, 4, 6, 8, 10$) system.

Type of bond	Covalence character C_C [%]
Ge-Se	92.96
Se-As	96.64
Se-Bi	93.21

3.5. Density, compactness, molar volume and some other relevant measurements

Theoretical density values were calculated using the relation, $\rho_{\text{th}} = (\sum x_i/d_i)^{-1}$, deduced by Fayek et al. [48], where x_i is the weight fraction and d_i is the density of the structural unit and are reported in Table 5. It is evident from the Table that density increases with the addition of Bi content to the a-Ge-Se-As-Bi alloy. The empirical equation

of the density variation with Bi content is given as; $\rho = 4.96 + 0.027x$ gm/cc, where x is Bi at.%. This behavior of density can be ascribed to the fact that density and the atomic mass of Bi are larger than that of replaced Se atoms. The system physical density increases and further accounts for the rise in the refractive index. This may be attributed to the increase in polarizability linked with the larger Bi atom according to Lorentz-Lorentz relation:

$$\frac{n^2 - 1}{n^2 + 2} = \frac{1}{3\epsilon_0} \sum_i N_i \alpha_{pi} \quad (12)$$

where ϵ_0 is the vacuum permittivity, N_i is the number of polarizable units of i type per unit volume with polarizability, α_{pi} . An increase in atomic radius of an atom leads to an increase in polarizability and, in turn, results in the increase in refractive index [49]. The atomic radius of Se is 1.16 Å and Bi is 1.46 Å.

Packing density is defined as the ratio of the used space to the allocated space. It was determined using the formula:

$$\text{Packing density} = \frac{N_A \cdot \rho}{M} \quad (13)$$

where N_A is Avogadro number and M is the molecular weight [24]. The formulated values of packing density are given in Table 5. Decrease in the packing density with an increase in Bi content results due to the subsequent increase in glass density.

The molar volume (V_m) of the multi-component chalcogenide system was determined from the theoretical density data by the equation:

$$(V_m) = \frac{1}{\rho} \sum_i x_i M_i \quad (14)$$

where M_i is the molecular weight of the i^{th} component and x_i is the atomic percentage of the same element in the sample. The values of molar volume with composition are tabulated in Table 5. It is clear that the values of molar volume increase with an incorporation of Bi in the parent alloy and so is the density. It is expected that the molar volume should show an opposite behavior compared to density. However, this anomalous behavior was reported earlier for many semiconductors [50, 51]. This trend supports the so-called open structure concept [52].

The compactness δ is a measure of the normalized change of the mean atomic volume due to chemical interactions of the elements forming the network of a given solid [32]. Therefore, it is more sensitive to changes in structure of the glass network as compared to mean atomic volume. It is also associated with the free volume and flexibility of this network [53]. It was calculated from the relation [54]:

$$\delta = \frac{\sum_i \frac{c_i A_i}{\rho_i} - \sum_i \frac{c_i A_i}{\rho}}{\sum_i \frac{c_i A_i}{\rho}} \quad (15)$$

where c_i is the atomic fraction, A_i is the atomic weight, ρ_i is the atomic density of the i^{th} element of the glass and ρ is the measured density of the glass. Table 5 summarizes the density of the investigated compositions and corresponding compactness. It is found that compactness decreases with an increase in Bi content. When Bi enters the Ge–As–Se system, it creates bonds with Se. New Se–Bi bonds with longer bond length (2.7 Å) are formed at an expense of Se–Se bonds (2.1 Å). Due to this, the atomic arrangements become less tightly bound. This causes an increase in the molar volume and consequent decrease in the compactness (Fig. 4) [32]. Also, values of compactness are negative, which corresponds to a larger free volume and flexibility [47].

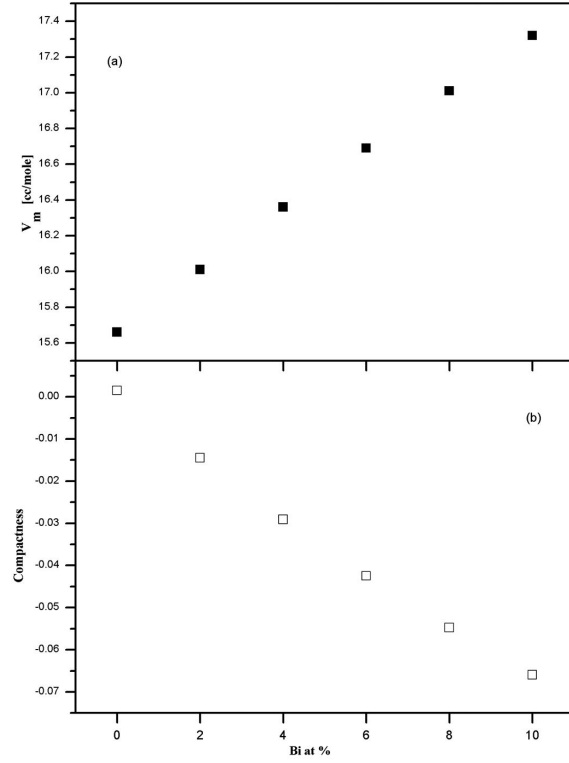


Fig. 4. Variation of (a) molar volume and (b) compactness with Bi at.%; for $\text{Ge}_{12}\text{Se}_{76-x}\text{As}_{12}\text{Bi}_x$ ($x = 0, 2, 4, 6, 8, 10$) glassy alloys.

The free volume percentage FVP in the glass was calculated using the relation [55]:

$$FVP = \frac{V_m - V_T}{V_m} 100\% \quad (16)$$

where V_T is the theoretical molar volume. The calculation of V_T for the composition $\text{Ge}_{12}\text{Se}_{76-x}\text{As}_{12}\text{Bi}_x$ was made using the following additive formula:

$$V_T = 12V(\text{Ge}) + (76 - x)V(\text{Se}) + 12V(\text{As}) + xV(\text{Bi}) \quad (17)$$

where $V(\text{Ge})$, $V(\text{Se})$, $V(\text{As})$ and $V(\text{Bi})$ are the atomic volumes of elements Ge, Se, As and Bi, respectively. The results are shown in Table 5. FVP is increasing with the addition of Bi content. These changes are presumably caused by the mechanical and chemical thresholds, respectively [55]. Consequent changes also occur in the number of bonds per unit volume of the glassy network. The changes

Table 5. Values of density (ρ), packing density, molar volume (V_m), compactness (δ), free volume percentage (FVP), excess volume (V_e) and M values for $\text{Ge}_{12}\text{Se}_{76-x}\text{As}_{12}\text{Bi}_x$ ($x = 0, 2, 4, 6, 8, 10$) system.

x	ρ [g/cc]	Packing density $\times 10^{22}$	V_m [cc/mol]	δ	FVP	V_e [cc/mol]	M [g/mol]
0	4.96	3.85	15.66	0.00149	0.15	-0.02	77.72
2	5.02	3.76	16.01	-0.01447	1.45	0.23	80.32
4	5.07	3.68	16.36	-0.02910	2.91	0.48	82.91
6	5.12	3.61	16.69	-0.04250	4.25	0.71	85.52
8	5.18	3.54	17.01	-0.05476	5.48	0.93	88.11
10	5.24	3.48	17.32	-0.06597	6.59	1.14	90.71

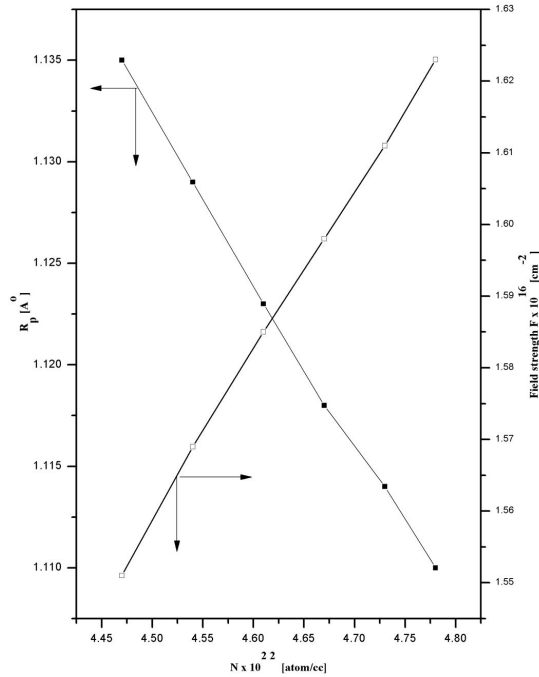


Fig. 5. Variation of (a) polaron radius [R_p in Å] and (b) field strength [$F \times 10^{16} \text{ cm}^{-2}$] with Se atomic density [$N \times 10^{22}$] for $\text{Ge}_{12}\text{Se}_{76-x}\text{As}_{12}\text{Bi}_x$ ($x = 0, 2, 4, 6, 8, 10$) glassy alloys.

in FVP are due to the modification in the composition structure induced by the variation in interatomic spacing.

The excess volume (V_e) was calculated using the following relation:

$$V_e = V_m - \sum_i x_i V_m(i) \quad (18)$$

where x_i is the molar fraction of the sample and $V_{m(i)}$ is the molar volume of each component.

The values of the excess volume are also given in Table 5. Most of the compositions show positive values for V_e also implying loosely packed structures. This is in fair agreement with the change in compactness values and the results reported by other workers on semiconducting glassy matrix [56].

The polaron concept has been studied in both ordered and disordered solids. A polaron is a quasi-particle used to comprehend the interactions between electrons and atoms in solid materials. The general notion of a polaron can also be extended to describe other interactions between the electrons and ions. The polaron radius R_p (i) must be greater than the radius of the atom on which the electron is localized and (ii) less than the distance r , separating atomic sites. The size of the polaron is found to decrease as the number of atoms increases [35]. The polaron radius R_p and the field strength, (F) were determined by the following relations [57]:

$$R_p = \frac{1}{2} \left(\frac{\pi}{6\dot{N}} \right)^{1/3} \quad (19)$$

and

$$F = \left(\frac{V_{No.}}{R_p^2} \right) \quad (20)$$

where $V_{No.}$ is the valence number of Se element and \dot{N} is Se atomic density existing in the system. \dot{N} was calculated using the Naster-Kingery formula [58]:

$$\dot{N} = \frac{\rho_s W_p N_A}{AW \times 100} \quad (21)$$

where ρ_s is the sample density, N_A is Avogadro number, AW is the atomic weight of Se and W_p is the weight percent of the Se content in the glassy matrix. Also the average spacing of Se–Se or the interatomic distance r was calculated using the equation, $r = (1/\dot{N})^{1/3}$.

Table 6. Values of average spacing (r), polaron radius (R_p), field strength (F) and N for $\text{Ge}_{12}\text{Se}_{76-x}\text{As}_{12}\text{Bi}_x$ ($x = 0, 2, 4, 6, 8, 10$) system.

x	r [Å]	R_p [Å]	$F \times 10^{16}$ [cm ⁻²]	$\dot{N} \times 10^{22}$ [atom/cc]
0	2.817	1.135	1.551	4.47
2	2.802	1.129	1.569	4.54
4	2.788	1.123	1.585	4.61
6	2.775	1.118	1.598	4.67
8	2.764	1.114	1.611	4.73
10	2.755	1.110	1.623	4.78

The formulated values of \dot{N} , the average spacing, polaron radius and the field strength are given in Table 6. Average spacing and polaron radius are found to decrease, whereas an increase is observed in field strength and Se atomic density values. Fig. 5 shows a decrease in the polaron radius and an increase in field strength with increasing Se atomic density. Therefore, this decrease in R_p , with the increase in Bi, is presumably due to the increase in the number density \dot{N} . This decrease also suggests an increase in free space within the glass structure, compared with previously calculated compactness values. The decrease in compactness values indicates loosely packed glassy matrix. From the tabulated values, it is clearly seen that the average spacing is also decreasing with an increase in Bi content. In chalcogenide glasses, the energy of the conduction band edge is decided by the number of atoms per unit volume \dot{N} [48]. An increase in \dot{N} values in the system under observation, leads to presumable decrease in the energy of conduction band edge, which further accounts for the observed lowering in the band gap with the Bi addition.

4. Conclusion

Many of the physical properties of Ge–Se–As–Bi glassy alloys were studied and discussed. The average coordination number, total number of constraints, density, molar volume, field strength, number density, mean bond energy, glass transition temperature were found to increase with an increase in Bi content. A linear relationship was found between $\langle E \rangle$ and T_g and reached a maximum at the chemical threshold when $R \approx 1$. On the contrary, lone pair electrons, cohesive energy, theoretical band gap, electronegativity, an average heat of atomization, compactness, polaron radius, the energy of conduction band were found to decrease with an increase in Bi content. The results were interpreted in terms of bond strength, defects states, and chemical bond approach model. Physical parameters were sensitive to changes in composition and could be tunable for specific optical, electrical, mechanical and thermal applications etc. Thus, an understanding of the physical parameters for $\text{Ge}_{12}\text{Se}_{76-x}\text{As}_{12}\text{Bi}_x$ ($x = 0, 2, 4, 6, 8, 10$) lone pair semiconductor was achieved. The substantial matter of further research on the effect of Bi addition in this semiconductor glassy system would include various experimental characterizations to validate theoretical data.

References

- [1] KAMIYA T., TSUCHIYA M., *Jpn. J. Appl. Phys.*, 44 (2005), 5875.
- [2] EGGLETON B.J., LUTHER-DAVIS B., RICHARDSON K., *Nat. Photonics*, 5 (2011), 141.
- [3] SÁMSON Z.L., YEN S.C., MAC-DONALD K.F., KNIGHT K., *Phys. Status Solidi-R*, 4 (2010), 274.
- [4] AKSHATHA W.A.G.H., RAVIPRAKASH Y., AJITHKUMAR M.P., UPADHYAYA V., KAMATH S.D., *T. Nonferr. Metal. Soc.*, 25 (2015), 1185.
- [5] TANAKA K., SHIMAKAWA K., *Amorphous chalcogenide semiconductors and related materials*, Springer Science & Business Media, 2011.
- [6] WANG F., ZHANG Z., LIU R., WANG X., ZHU X., PAN A., ZOU B., *Nanotechnology*, 18 (2007), 305705.
- [7] SARRACH J., NEUFVILLE DE J.P., HAWORTH W.L., *J. Non-Cryst. Solids*, 22 (1976), 245.
- [8] SHARMA I., TRIPATHI S.K., BARMAN P.B., *J. Phys. D Appl. Phys.*, 40 (2007), 4460.
- [9] SHARMA I., TRIPATHI S.K., MONGA A., BARMAN P.B., *J. Non-Cryst. Solids*, 354 (2008), 3215.

- [10] CALVEZ L., YANG Z., LUCAS P., *Phys. Rev. Lett.*, 101 (2008), 177402.
- [11] GOPINATH J.T., SOLJACIC M., IPPEN E.P., FUFLYGIN V.N., KING W.A., SHURGALIN M., *J. Appl. Phys.*, 96 (2004), 6931.
- [12] NICHOLSON J.W., YAN M.F., WISK P., FLEMING J., DIMARCELLO F., MONBERG E., YABLON A., JØRGENSEN C., VENG T., *Opt. Lett.*, 28 (2003), 643.
- [13] QUOCHI F., DINU M., PFEIFFER L.N., WEST K.W., KERBAGE C.E., WINDERLER R.S., EGGELETON B.J., *Phys. Rev. B*, 67 (2003), 235323.
- [14] ZHA C., LUTHER-DAVIES B., WANG R., SMITH A., PRASAD A., JARVIS R.A., MADDEN S., RODE A., *ACOFI/AOS – Proceedings*, Melbourne, Australia, 2006.
- [15] MEHRA R.M., KOHLI S., PUNDIR A., SACHDEV V.K., MATHUR P.C., *J. Appl. Phys.*, 81 (1997), 7842.
- [16] XIA F., BACCARO S., WANG W., PILLONI L., ZHANG X., ZENG H., CHEN G., *J. Non-Cryst. Solids*, 354 (2008), 1137.
- [17] THOMAS S., PHILIP J., *Solid State Commun.*, 107 (1998), 423.
- [18] TOHGE N., MINAMI T., YAMAMOTO Y., TANAKA M., *J. Appl. Phys.*, 51 (1980), 1048.
- [19] SAXENA M., GUPTA S., *IJECE*, 3 (2013), 76.
- [20] SHARMA I., KUMAR A., TRIPATHI S.K., BARMAN P.B., *J. Phys. D Appl. Phys.*, 41 (2008), 175504.
- [21] EL-KORASHY A., EL-KABANY N., EL-ZAHED H., *Physica B*, 365 (2005), 55.
- [22] IOFFE A.F., REGEL A.R., *Prog. Semicond.*, 4 (1960), 237.
- [23] FOUAD S.S., *J. Phys. D Appl. Phys.*, 28 (1995), 2318.
- [24] PAMUKCHIEVA V., SZEKERES A., TODOROVA M., SVAB E., REVAY Z.S., SZENTMIKLOSI L., *J. Non-Cryst. Solids*, 355 (2009), 2485.
- [25] PHILLIPS J.C., *J. Non-Cryst. Solids*, 34 (1979), 153.
- [26] THORPE M.F., *J. Non-Cryst. Solids*, 57 (1983), 355.
- [27] PAULING L., *The Nature of the Chemical Bond*, Cornell University Press, Ithaca, NY, 1960.
- [28] FOUAD S.S., FAYEK S.A., ALI M.H., *Vacuum*, 49 (1998), 25.
- [29] LIANG Z., *J. Non-Cryst. Solids*, 127 (1991), 298.
- [30] SINGH A.K., MEHTA N., SINGH K., *Philos. Mag. Lett.*, 90 (2010), 201.
- [31] THORPE M.F., TICHÝ L., *Properties and applications of amorphous materials*, Springer Science & Business Media, 2012.
- [32] TICHÝ L., TICHÁ H., *J. Non-Cryst. Solids*, 189 (1995), 141.
- [33] FOUAD S.S., EL-BANA M.S., SHARMA P., SHARMA V., *Appl. Phys. A*, 120 (2015), 137.
- [34] EL GHANI H.A., EL RAHIM M.A., WAKKAD M.M., SEHLI A.A., ASSRAAN N., *Physica B*, 381 (2006), 156.
- [35] HASSANIEEN A.S., AKL A.A., *J. Alloy. Compd.*, 648 (2015), 280.
- [36] FARAG A.A.M., RAFAE M.A., ROUSHDY N., EL-SHAZLY O., EL-WAHIDY E.F., *J. Alloy. Compd.*, 621 (2015), 434.
- [37] BICERANO J., OVSHINSKY S. R., *J. Non-Cryst. Solids*, 74 (1985), 75.
- [38] SHAABAN E.R., KANSAL I., MOHAMED S.H., FERRIERA J.M.F., *Physica B*, 404 (2009), 3571.
- [39] SHAABAN E.R., EL-SHAikh H.A., SORAYA M.M., *Optoelectron. Adv. Mat.*, 9 (2015), 587.
- [40] SANDERSON R.T., *Inorganic Chemistry*, Affiliated East-West Press, New Delhi, 1971.
- [41] MOTT N.F., DAVIS E.A., *Electronics Process in Non-Crystalline Materials*, Oxford University Press, Clarendon, 1971.
- [42] KHAN M.A.M., ZULFEQUAR M., HUSAIN M., *Opt. Mater.*, 22 (2003), 21.
- [43] DAHSHAN A., ALY K.A., *Philos. Mag.*, 88 (2008), 361.
- [44] KASTNER M., *Phys. Rev. B*, 7 (1973), 5237.
- [45] BENOIT C., AIGRAIN P., BALKANSHI M., *Selected Constants Relative to Semiconductors*, Pergamon Press, New York, 1961.
- [46] HASANIEEN A.S., AKL A.A., *Superlattice. Microst.*, 89 (2016), 153.
- [47] SHARMA A., MEHTA N., *Mater. Chem. Phys.*, 161 (2015), 35.
- [48] FAYEK S.A., BALBOUL M.R., MARZOUK K.H., *Thin Solid Films*, 515 (2007), 7281.
- [49] ELLIOTT S.R., *The Physics and Chemistry of Solids*, Wiley, Chichester, 2000.
- [50] AKL A.A., HASSANIEEN A.S., *Superlattice. Microst.*, 85 (2015), 67.
- [51] HASSANIEEN A.S., AKL A.A., *J. Non-Cryst. Solids*, 428 (2015), 112.
- [52] FAROUK M., SAMIR A., METAWE F., ELOKR M., *J. Non-Cryst. Solids*, 371 (2013), 14.
- [53] SHARMA, I., *J. Optoelectron. Adv. M.*, 14 (2012), 483.
- [54] VLČEK M., FRUMAR M., *J. Non-Cryst. Solids*, 97 (1987), 1223.
- [55] SHARDA S., SHARMA N., SHARMA P., SHARMA V., *J. Non-Cryst. Solids*, 362 (2013), 136.
- [56] NANDA K., KUNDU R.S., SHARMA S., MOHAN D., PUNIA R., KISHORE N., *Solid State Sci.*, 45 (2015), 15.
- [57] BOOTJOMCHAI C., *Radiat. Phys. Chem.*, 110 (2015), 96.
- [58] NASTER H.H., KINGERY W.D., *Proceedings of the Seventh International Conference on Glass, Brussels*, Gordon and Breach, New York, 1965.

Received 2016-08-16

Accepted 2018-01-20